

Statistical mechanics of membranes: freezing, undulations, and topology fluctuations

This article has been downloaded from IOPscience. Please scroll down to see the full text article.

2000 J. Phys.: Condens. Matter 12 A29

(<http://iopscience.iop.org/0953-8984/12/8A/304>)

View [the table of contents for this issue](#), or go to the [journal homepage](#) for more

Download details:

IP Address: 129.252.86.83

The article was downloaded on 27/05/2010 at 11:26

Please note that [terms and conditions apply](#).

Statistical mechanics of membranes: freezing, undulations, and topology fluctuations

G Gompper^{†‡} and D M Kroll[§]

[†] Institut für Festkörperforschung, Forschungszentrum Jülich, 52425 Jülich, Germany

[‡] Max-Planck-Institut für Kolloid- und Grenzflächenforschung, Am Mühlenberg, Haus 2, 14476 Golm, Germany

[§] Department of Medicinal Chemistry and Minnesota Supercomputer Institute, University of Minnesota, 308 Harvard Street SE, Minneapolis, MN 55455, USA

Received 10 September 1999

Abstract. Membranes are two-dimensional sheets of molecules which are embedded and fluctuate in three-dimensional space. The shape and out-of-plane fluctuations of tensionless membranes are controlled by their bending rigidity. Due to their out-of-plane fluctuations, flexible membranes exhibit very different behaviour to flat two-dimensional systems. We discuss three properties of membranes: (i) the renormalization of the bending rigidity in fluid membranes due to undulations on short length scales; (ii) the suppression of the crystalline phase, and the hexatic-to-fluid transition; and (iii) the lamellar-to-sponge transition in systems with variable topology. We focus on simulation studies, which are based on the numerical analysis of dynamically triangulated surface models.

1. Introduction

1.1. Amphiphilic bilayer membranes

Amphiphilic molecules of sufficiently long chain length and similar head and tail sizes spontaneously self-assemble in an aqueous environment into bilayers. In this arrangement, the sheet of head-groups shields the hydrocarbon core of the bilayer from contact with water. For long-chain amphiphiles, the molecular solubility in water is very small, so essentially all amphiphilic molecules are part of a bilayer. In this case, the area of the bilayer—or membrane—is determined by the amphiphile volume fraction, so the elastic constant which controls the shape and fluctuations of the membrane is not the interfacial tension, but the bending rigidity κ of the thin amphiphile sheet. The curvature energy of a fluid membrane is usually written in the form (Helfrich 1973, Canham 1970)

$$\mathcal{H} = \int dS \left[\frac{\kappa}{2} (c_1 + c_2)^2 + \bar{\kappa} c_1 c_2 \right] \quad (1)$$

where c_1 and c_2 are the two principal curvatures at each point of the membrane, and the integral extends over the whole membrane area. The second contribution in equation (1) is related by the Gauss–Bonnet theorem to the Euler characteristic:

$$\chi_E = \frac{1}{2\pi} \int dS c_1 c_2 \quad (2)$$

which counts the number of disconnected components minus the number of handles of a surface without holes:

$$\chi_E = 2(\text{No of components} - \text{No of handles}). \quad (3)$$

In thermal equilibrium, the phase behaviour of a membrane ensemble is determined by the amphiphile volume fraction ϕ and by the elastic constants κ and $\bar{\kappa}$. The phases which are typically observed in these systems are the lamellar phase, the sponge phase or the cubic bicontinuous—or plumber's nightmare—phase, and a phase of (small) vesicles or micelles. These phases are characterized by $\chi_E \simeq 0$, $\chi_E \ll 1$, and $\chi_E \gg 1$, respectively.

It is also possible to investigate the shapes and fluctuations of giant vesicles, which are only metastable, but which have lifetimes of hours or days (Lipowsky and Sackmann 1995, Seifert 1997). In this case, not only the area but also the enclosed volume—whose value is determined by the small amount of ionic solute in the water which cannot penetrate the membrane—is conserved. Furthermore, the area difference between the inner and the outer layers of the membrane may be conserved due to the slow flip-flop of amphiphilic molecules between these layers. This opens a whole universe of shapes and shape transitions, which has been reviewed in detail by Lipowsky and Sackmann (1995) and Seifert (1997) recently.

At low temperatures, the membrane freezes into a crystalline state. In this case, the membrane attains a finite shear modulus, and terms for the in-plane shear elasticity have to be added to the curvature energy (1). In fact, it has been argued (Seung and Nelson 1988, Nelson 1996) that the energy of dislocations is so small in flexible membranes that these topological defects always destroy the long-range translational order in membranes which are much larger than the buckling radius

$$R_b \simeq 120 \frac{\kappa}{K_0 a} \quad (4)$$

where K_0 is the two-dimensional Young modulus, and a is a molecular length scale. The low-temperature phase of membranes in which the amphiphiles are *not* chemically linked is therefore expected to be a hexatic phase, with short-range translational, but (quasi-) long-ranged bond-orientational order.

1.2. Network models of membranes

Membranes are very soft materials, and thus often have large thermal fluctuations. Monte Carlo simulations are therefore an important tool for investigating the thermal properties and phase behaviour of individual membranes and membrane ensembles. These simulations are based on triangulated surfaces (Gompper and Kroll 1997a, d). There are four fundamentally different classes of triangulated surface models. Fixed-connectivity models have finite in-plane shear modulus, and can therefore be used to model systems like polymerized membranes (Kantor *et al* 1986) or thin elastic sheets (Lobkovsky *et al* 1995, Zhang *et al* 1995, Kramer and Witten 1997, Lobkovsky and Witten 1997). Dynamically triangulated surfaces, on the other hand, allow for diffusion within the surface and are appropriate models for systems like fluid membranes. Models which allow for both in-plane diffusion and topological fluctuations in the membrane structure can be used to study microemulsions and sponge phases (Gompper and Kroll 1998) and vesicle size distributions. Finally, dynamically triangulated surfaces with holes (Shillcock and Boal 1996, Shillcock and Seifert 1998) can be used to model the membranes with open edges, and therefore the pore formation and rupturing of membranes.

The purpose of this paper is to review recent work on the freezing of membranes and vesicles, the sponge-to-lamellar transition in ensembles of fluctuating topology, and the undulation modes of fluid vesicles. Earlier work, in particular on the behaviour of polymerized

membranes, has been reviewed in references (Gompper and Kroll 1997a, d), and will not be discussed here.

2. Undulations of fluid membranes and vesicles

In the limit of large bending rigidities, $\kappa/k_B T \gg 1$, the spectrum of thermally excited undulation modes of a quasi-spherical vesicle can be calculated analytically (Helfrich 1986, Milner and Safran 1987). The vesicle shape in polar coordinates is expanded in a series of spherical harmonics:

$$r(\Omega) = r_0 + \sum_{l=1}^{l_M} \sum_{m=-l}^l a_{lm} Y_{lm}(\Omega) \quad (5)$$

where r_0 is the average vesicle radius. The fluctuation amplitudes are then found to be

$$\langle a_{lm}^2 \rangle = \frac{k_B T r_0^2}{\kappa} \frac{1}{l(l+1)(l-1)(l+2)}. \quad (6)$$

For smaller bending rigidities, the undulation modes begin to interact, which leads to a scale-dependent, renormalized bending rigidity (Peliti and Leibler 1985, Helfrich 1985):

$$\kappa^{(R)}(\ell)/k_B T = \kappa/k_B T - \frac{\alpha}{4\pi} \ln(\ell/a) \quad (7)$$

where a is a microscopic length. The universal amplitude α has been predicted to have the value $\alpha = 3$ (Peliti and Leibler 1985, Kleinert 1986, Cai *et al* 1994), $\alpha = 1$ (Helfrich 1985), or $\alpha = -1$ (Helfrich 1998).

Monte Carlo simulations have been used to decide which of these predictions is correct. The simplest quantity to study is the average volume $\langle V \rangle$ of a vesicle as a function of its area A and bending rigidity (Gompper and Kroll 1995, Ipsen and Jeppesen 1995). This analysis provides evidence for $\alpha = 3$. However, it is hampered by the fact that the reduced volume $\langle V \rangle A^{-3/2}$ is not simply a function of the dimensionless ratio of the two length scales, the vesicle radius, \sqrt{A} , and persistence length, $\xi_p = a \exp[(4\pi/\alpha)\kappa/k_B T]$, but that logarithmic corrections to the scaling are expected (Gompper and Kroll 1996).

Therefore, we have employed simulations recently to study the undulation spectra of quasi-spherical vesicles (Gompper and Kroll 1999). In such an analysis, the renormalized rigidity is obtained from a fit of the numerically determined fluctuation amplitudes $\langle a_{lm}^2 \rangle$ to the spectrum (6), with κ replaced by κ_{eff} as fitting parameter. Preliminary results for the effective rigidity, κ_{eff} , indicate that κ_{eff} decreases with increasing vesicle size A , so α is positive.

3. Freezing of membranes

3.1. Freezing of membranes in two dimensions

Models of self-avoiding fluid membranes are usually constructed by placing hard spheres at each vertex of a triangulated surface and connecting neighbouring vertices by a tethering potential. In *two space dimensions*, the behaviour of this type of network resembles that of a gas of hard spheres (Strandburg 1986, Zollweg *et al* 1989, Lee and Strandburg 1992, Zollweg and Chester 1992), the primary difference being that the average density is now determined by the tether length rather than an external pressure. Dynamically triangulated surfaces should therefore undergo a freezing transition with decreasing tether length. Such a transition has indeed been observed in Monte Carlo simulations (Gompper and Kroll 1997c).

Nelson and Halperin (1979) and Young (1979) have shown that the transition between a two-dimensional solid and the isotropic liquid can occur via two continuous transitions. According to the Kosterlitz–Thouless–Halperin–Nelson–Young (KTHNY) scenario, the two-dimensional solid, which has quasi-long-range translational order and true long-range bond-orientational order, first melts via a dislocation-unbinding transition to a hexatic phase with short-range translational order and quasi-long-range bond-orientational order. Subsequently, at a higher temperature, disclinations proliferate, causing a transition to the isotropic fluid phase characterized by short-range translational and bond-orientational order. It is also possible that a first-order transition takes the crystal directly into the fluid phase.

There has been a considerable computational effort to verify the KTHNY predictions for specific model systems. While some studies support the KTHNY scenario (Zollweg and Chester 1992, Naidoo and Schnitker 1994, Chen *et al* 1995, Bagchi *et al* 1996, Fernández *et al* 1997, Jaster 1998), a comparable number conclude that the transition is first order (Lee and Strandburg 1992, Weber *et al* 1995), so there is no consensus regarding the character of the transition. Indeed, it has proven to be extremely difficult to discriminate between a weak first-order transition and the KTHNY scenario, with a very narrow region of hexatic phase.

On a phenomenological level, an unusual property of the network model that we study is that in contrast to atomistic models, the average area of the network *decreases* on melting (Gompper and Kroll 2000). In atomistic models, most of the area increase upon melting is due to the creation of ‘geometrical voids’, which are not possible in a network model due to the constraint of a fixed tether length, rather than an increase in the most probable nearest-neighbour spacing (Glaser and Clark 1993). In fact, the most probable nearest-neighbour distance actually decreases slightly upon melting—in accordance with our results for the network model. Another consequence of this suppression of density fluctuations is that the tethered fluid freezes at a significantly lower density than the hard-sphere fluid.

To characterize the order of the transition, we have studied the finite-size scaling behaviour of the translational and hexatic order parameters and susceptibilities. The results of this scaling analysis are consistent with the existence of two transitions, with a very narrow interval of tether lengths, over which the hexatic phase is stable (Gompper and Kroll 2000).

3.2. Freezing of flexible membranes

When membranes are allowed to buckle out of plane, the elastic energy of topological defects like dislocations and disclinations is reduced (Seung and Nelson 1988). This is most easily seen for a fivefold disclination. In the case of flat membranes, the standard theory of elasticity yields the stretching energy

$$E_s = \frac{K_0 s^2}{32\pi} R^2 \quad (8)$$

for a membrane patch of radius R , where K_0 is again the two-dimensional Young modulus and s is the strength of the disclination, defined as the angle in radians of the wedge which must be removed or added to a perfect crystal to make the defect. On the other hand, the membrane can buckle into a cone for $s > 0$, which does not cost *any* stretching energy, but has the bending energy

$$E_b = s\kappa \ln(R/a). \quad (9)$$

Thus, a disclination will be flat for R smaller than the buckling radius

$$R_b \simeq 10 \left(\frac{\kappa}{K_0 s} \right)^{1/2} \quad (10)$$

which is the radius where the stretching and bending energies of equations (8) and (9) become comparable. Only for $R > R_b$ is the buckled membrane energetically more favourable than the flat state.

Similarly, buckling reduces the elastic energy of dislocations. Seung and Nelson (1988) give strong numerical evidence that the dislocation energy no longer increases logarithmically with R , as in the flat state, but approaches a constant for $R \rightarrow \infty$ in this case. A Peierls argument then shows immediately that dislocations should destabilize the crystalline phase at any finite temperature. The phase diagram as a function of bending rigidity and hexatic stiffness can then be obtained from a detailed renormalization-group analysis (Park and Lubensky 1996b, a).

3.3. Freezing of flexible vesicles

The freezing of flexible vesicles proceeds very much like the freezing of flexible planar membranes. The free energy of dislocations is again expected to be finite, with the result that these defects destroy the crystalline order at low temperatures. Monte Carlo simulations of the network model for fluid membranes with spherical topology nicely confirm this picture (Gompper and Kroll 1997b, c). A typical configuration of topological defects is shown in figure 1. For this small tether length, in the hexatic phase, a number of free dislocations can be seen. More quantitatively, it has been possible to determine the scaling form of the dislocation free energy from the simulations.

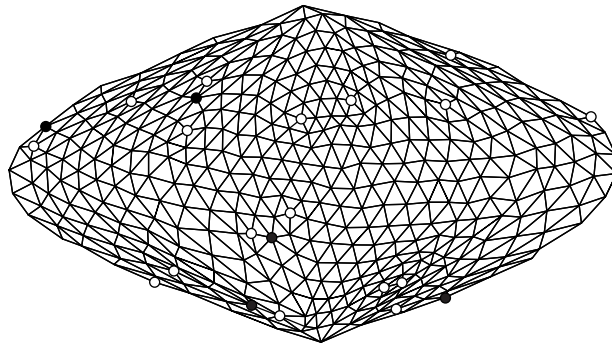


Figure 1. The distribution of disclinations on a flexible vesicle for tether lengths $l_0 = 1.33$. Fivefold and sevenfold disclinations are shown by open (○) and closed (●) circles, respectively.

The resulting phase diagram, shown in figure 2, is in qualitative agreement with that of Park and Lubensky (1996a), when the hexatic stiffness K_H (which we cannot determine easily) is assumed to be proportional to the Young modulus of a polymerized network with the same tether length. In particular, a transition from the hexatic to the fluid can be induced by decreasing the bending rigidity.

However, there is an important difference between vesicles and planar membranes. It has been argued by Park (1996) that shape fluctuations of spherical vesicles cause disclinations to be screened at length scales larger than $R(\kappa/K_H)^{1/2}$, where R is the radius of the vesicle. Therefore, there are unbound disclinations at all non-zero temperatures, and strictly speaking, the hexatic phase does not exist, although there may still be a sharp crossover in many quantities—as observed in the simulations (Gompper and Kroll 1997b, c)—which has been used to determine the location of the effective transition line in figure 2.

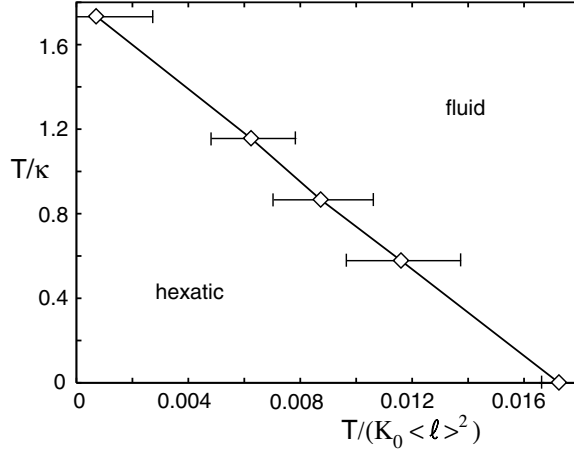


Figure 2. The phase diagram of flexible vesicles as a function of the reduced bending rigidity κ/T and reduced Young modulus $(K_0\langle l \rangle^2)/T$, where $\langle l \rangle$ is the average bond length. The solid line is a guide to the eye.

4. Membrane ensembles with fluctuating topology

In order to see the limits of stability of the lamellar phase of fluid membranes, it is convenient to rewrite the curvature Hamiltonian (1) in the form

$$\mathcal{H} = \int dS \left[\frac{\kappa_+}{2} (c_1 + c_2)^2 + \frac{\kappa_-}{2} (c_1 - c_2)^2 \right] \quad (11)$$

where $\kappa_+ = \kappa + \bar{\kappa}/2$ and $\kappa_- = -\bar{\kappa}/2$. The lamellar phase can only be stable for $\kappa_+ > 0$ and $\kappa_- > 0$, i.e. for $\kappa > 0$ and $-2\kappa < \bar{\kappa} < 0$. Here, $\kappa_+ = 0$ is the line of instabilities towards a phase of small vesicles (with $c_1 \approx c_2$), and $\kappa_- = 0$ towards a plumber's-nightmare-like phase (with $c_1 \approx -c_2$). However, this argument ignores the thermal fluctuations of the membranes, which lead to a renormalization of κ (compare equation (7)) and $\bar{\kappa}$ (David 1989), such that

$$\kappa_{\pm}^{(R)}(\ell)/k_B T = \kappa_{\pm}/k_B T - \frac{\alpha_{\pm}}{4\pi} \ln(\ell/a) \quad (12)$$

where $\alpha_+ = 4/3$ and $\alpha_- = 5/3$. The typical length scale ℓ/a in this case is proportional to the inverse amphiphile volume fraction $\phi^{-1} = V/(aA)$. The stability limits are now given by $\kappa_{\pm}^{(R)}(\phi_0/\phi) = 0$, where ϕ_0 is a constant of order unity. Therefore, in a phase diagram (Morse 1994, Golubović 1994, Morse 1997) of $\ln(\phi)$ versus $\bar{\kappa}$, the lamellar phase occupies a V-shaped region centred at $\bar{\kappa} \simeq -\kappa$. The lamellar-to-sponge transition, in particular, is predicted to be located near the line

$$\ln(\phi/\phi_0) = \frac{2\pi}{\alpha_-} \frac{\bar{\kappa}}{k_B T}. \quad (13)$$

This phase transition is therefore a direct consequence of the $\bar{\kappa}$ -renormalization.

The renormalization of the curvature rigidities in equation (1) also affects the osmotic pressure p of the sponge phase. It has been argued by Roux *et al* (1990), Roux *et al* (1992), and Porte *et al* (1991) that the scale invariance of the curvature energy together with the logarithmic renormalization of κ and $\bar{\kappa}$ implies an equation of state of the form

$$pa^3/k_B T \equiv \frac{1}{k_B T} [\phi \partial f / \partial \phi - f] = [A(\kappa/k_B T, \bar{\kappa}/k_B T) + B(\kappa/k_B T, \bar{\kappa}/k_B T) \ln(\phi)] \phi^3 \quad (14)$$

where $f(\phi)$ is the free-energy density. Other forms of the osmotic pressure have also been suggested (Daicic *et al* 1995, Pieruschka and Safran 1995).

Monte Carlo simulations of a network model with fluctuating topology have been used to investigate both the lamellar-to-sponge transition and the properties of the sponge phase (Gompper and Kroll 1998). A typical configuration in the sponge phase is shown in figure 3. The characteristic, saddle-shaped geometry of the membrane is clearly visible, which leads to an Euler characteristic $\chi_E < 0$ (compare equation (3)). The numerical data for the osmotic pressure confirm the dependence (14), with $A(\bar{\kappa}/k_B T) = -(a_1 + a_2 \bar{\kappa}/k_B T)$ and $B(\bar{\kappa}/k_B T) \simeq 1$, where a_1 and a_2 are positive and of order unity (Gompper and Kroll 1998).

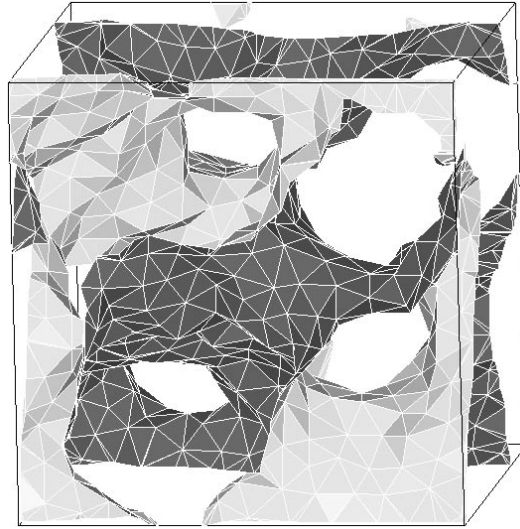


Figure 3. A typical membrane configuration in a sponge phase for bending rigidity $\kappa/k_B T \simeq 1.6$. The two sides of the membrane are shaded differently in order to emphasize the bicontinuous structure of this phase.

The simulation result for the phase diagram is shown in figure 4. The slope of the lamellar-to-sponge transition is found to be very close to the theoretical prediction (13) with $\alpha_- = 5/3$. This provides strong evidence for the presence of the logarithmic renormalization of $\bar{\kappa}$. Furthermore, the coexistence line of the sponge phase with an almost pure water phase is found to run roughly parallel to the lamellar instability line.

5. Summary and forward look

Simulation studies of dynamically triangulated surface models allow a detailed test of theoretical predictions for the behaviour of membranes. In this short review, we have focused on the renormalization of the bending rigidity, the freezing transition, and the sponge-to-lamellar transition. In all three cases, the simulation results clearly favour one of several conflicting theoretical predictions. Furthermore, simulations can be used to investigate membranes with small bending rigidities $\kappa/k_B T \simeq 1$, a regime which is outside the range of applicability of most analytical approaches.

Most of the simulations so far have been restricted to relatively simple systems. In the future, attention will certainly shift to more complicated systems with several components; these can be embedded in the membrane (Dan *et al* 1993, Kumar and Rao 1998), be attached

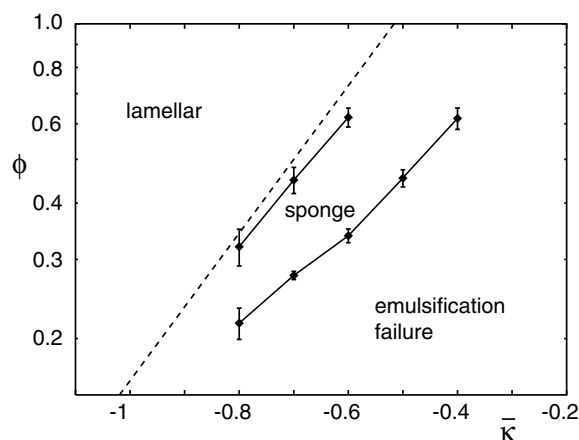


Figure 4. The phase diagram as a function of amphiphile concentration ϕ and saddle-splay modulus $\bar{\kappa}$, for $\kappa/k_B T \simeq 1.6$. Note the logarithmic scale of the abscissa. The dashed line shows the theoretical prediction (13) with $\alpha_- = 5/3$.

to or adsorbed into the membrane (Hiergeist *et al* 1996, Yaman *et al* 1997b), or be part of the solvent (Eisenriegler *et al* 1996, Yaman *et al* 1997a, Hanke *et al* 1999). Such models should begin to capture the complexity of real, biological membranes.

Acknowledgments

DMK acknowledges support from the National Science Foundation under Grant No DMR-9712134 and the donors of The Petroleum Research Fund, administered by the ACS.

References

- Bagchi K, Andersen H C and Swope W 1996 *Phys. Rev. E* **53** 3794
 Cai W, Lubensky T C, Nelson P and Powers T 1994 *J. Physique II* **4** 931
 Canham P B 1970 *J. Theor. Biol.* **26** 61
 Chen K, Kaplan T and Mostoller M 1995 *Phys. Rev. Lett.* **74** 4019
 Daicic J, Olsson U, Wennerström H, Jerke G and Schurtenberger P 1995 *J. Physique II* **5** 199
 Dan N, Pincus P and Safran S A 1993 *Langmuir* **9** 2768
 David F 1989 *Statistical Mechanics of Membranes and Surfaces* ed D Nelson, T Piran and S Weinberg (Singapore: World Scientific) pp 157–223
 Eisenriegler E, Hanke A and Dietrich S 1996 *Phys. Rev. E* **54** 1134
 Fernández J F, Alonso J J and Stankiewicz J 1997 *Phys. Rev. E* **55** 750
 Glaser M A and Clark N A 1993 *Adv. Chem. Phys.* **83** 543
 Golubović L 1994 *Phys. Rev. E* **50** R2419
 Gompper G and Kroll D M 1995 *Phys. Rev. E* **51** 514
 Gompper G and Kroll D M 1996 *J. Physique I* **6** 1305
 Gompper G and Kroll D M 1997a *Curr. Opin. Colloid Interface Sci.* **2** 373
 Gompper G and Kroll D M 1997b *Phys. Rev. Lett.* **78** 2859
 Gompper G and Kroll D M 1997c *J. Physique I* **7** 1369
 Gompper G and Kroll D M 1997d *J. Phys.: Condens. Matter* **9** 8795
 Gompper G and Kroll D M 1998 *Phys. Rev. Lett.* **81** 2284
 Gompper G and Kroll D M 1999 in preparation
 Gompper G and Kroll D M 2000 *Eur. Phys. J. B* at press
 Hanke A, Eisenriegler E and Dietrich S 1999 *Phys. Rev. E* **59** 6853

- Helfrich W 1973 *Z. Naturf.* c **28** 693
Helfrich W 1985 *J. Physique* **46** 1263
Helfrich W 1986 *J. Physique* **47** 321
Helfrich W 1998 *Eur. Phys. J. B* **1** 481
Hiergeist C, Indrani V A and Lipowsky R 1996 *Europhys. Lett.* **36** 491
Ipsen J H and Jeppesen C 1995 *J. Physique I* **5** 1563
Jaster A 1998 *Europhys. Lett.* **42** 277
Kantor Y, Kardar M and Nelson D R 1986 *Phys. Rev. Lett.* **57** 791
Kleinert H 1986 *Phys. Lett. A* **114** 263
Kramer E M and Witten T A 1997 *Phys. Rev. Lett.* **78** 1303
Kumar P B S and Rao M 1998 *Phys. Rev. Lett.* **80** 2489
Lee J and Strandburg K J 1992 *Phys. Rev. B* **46** 11 190
Lipowsky R and Sackmann E (ed) 1995 *Structure and Dynamics of Membranes—from Cells to Vesicles (Handbook of Biological Physics vol 1)* (Amsterdam: Elsevier)
Lobkovsky A, Gentges S, Li H, Morse D and Witten T A 1995 *Science* **270** 1482
Lobkovsky A and Witten T A 1997 *Phys. Rev. E* **55** 1577
Milner S T and Safran S A 1987 *Phys. Rev. A* **36** 4371
Morse D C 1994 *Phys. Rev. E* **50** R2423
Morse D C 1997 *Curr. Opin. Colloid Interface Sci.* **2** 365
Naidoo K J and Schnitker J 1994 *J. Chem. Phys.* **100** 3114
Nelson D R 1996 *Fluctuating Geometries in Statistical Mechanics and Field Theory* ed F David, P Ginsparg and J Zinn-Justin (Amsterdam: North-Holland) pp 423–77
Nelson D R and Halperin B I 1979 *Phys. Rev. B* **19** 2457
Park J M 1996 *Phys. Rev. E* **54** 5414
Park J M and Lubensky T C 1996a *Phys. Rev. E* **53** 2665
Park J M and Lubensky T C 1996b *Phys. Rev. E* **53** 2648
Peliti L and Leibler S 1985 *Phys. Rev. Lett.* **54** 1690
Pieruschka P and Safran S A 1995 *Europhys. Lett.* **31** 207
Porte G, Delsanti M, Billard I, Skouri M, Appell J, Marignan J and Debeauvais F 1991 *J. Physique II* **1** 1101
Roux D, Cates M E, Olsson U, Ball R C, Nallet F and Bellocq A M 1990 *Europhys. Lett.* **11** 229
Roux D, Coulon C and Cates M E 1992 *J. Phys. Chem.* **96** 4174
Seifert U 1997 *Adv. Phys.* **46** 13
Seung H S and Nelson D R 1988 *Phys. Rev. A* **38** 1005
Shillcock J C and Boal D H 1996 *Biophys. J.* **71** 317
Shillcock J C and Seifert U 1998 *Biophys. J.* **74** 1754
Strandburg K J 1986 *Phys. Rev. B* **34** 3536
Weber H, Marx D and Binder K 1995 *Phys. Rev. B* **51** 14 636
Yaman K, Pincus P and Marques C M 1997a *Phys. Rev. Lett.* **78** 4514
Yaman K, Pincus P, Solis F and Witten T A 1997b *Macromolecules* **30** 1173
Young A P 1979 *Phys. Rev. B* **19** 1855
Zhang Z, Davis H T, Maier R S and Kroll D M 1995 *Phys. Rev. B* **52** 5404
Zollweg J A and Chester G V 1992 *Phys. Rev. B* **46** 11 186
Zollweg J A, Chester G V and Leung P W 1989 *Phys. Rev. B* **39** 9518